

Research Article: New Research | Disorders of the Nervous System

Combined treatment With environmental enrichment And (-)-epigallocatechin-3-gallate ameliorates learning deficits And hippocampal alterations In A mouse model Of Down syndrome

Environmental Enrichment and (-)-Epigallocatechin-3-Gallate as a Therapy for DS

S. Catuara-Solarz 1,2,3 , J. Espinosa-Carrasco 1,2,4 , I. Erb 2,4 , K. Langohr 3,5 , J. R. Gonzalez 6,7 , C. Notredame 2,4 and M. Dierssen 1,3,8

¹Cellular & Systems Neurobiology, Systems Biology Program, the Barcelona Institute of Science and Technology, Centre for Genomic Regulation (CRG), Dr. Aiguader 88, 08003, Barcelona, Spain

DOI: 10.1523/ENEURO.0103-16.2016

Received: 2 May 2016
Revised: 26 August 2016
Accepted: 8 September 2016
Published: 19 October 2016

Authors Contribution: SCS designed research, performed research, analyzed data, wrote the paper; JEC, IE, KL, JRG analyzed data; CN supervised the PCA analysis, MD provided financial support, designed research, wrote the paper.

Funding: MINECO | Consejo Superior de Investigaciones Científicas (CSIC): 501100003339; SAF2013-49129-C2-1-R. DIUE of Generalitat de Catalunya (Grups consolidats): SGR 2014/1125. Fondation Jérôme Lejeune: N.A. CDTI Smartfoods, CIBER of Rare Disease ISCIII initiave: N.A.. EU-Era Net Neuron: PCIN-2013- 060. Severo Ochoa Center of Excellence: SEV- 2012-0208.

Conflict of Interest: Authors report no conflict of interest.

MINECO | Consejo Superior de Investigaciones Científicas (CSIC) [SAF2013-49129-C2-1-R], DIUE of Generalitat de Catalunya (Grups consolidats) [SGR 2014/1125], Fondation Jérôme Lejeune, CDTI Smartfoods, CIBER of Rare Disease ISCIII initiave, EU-Era Net Neuron [PCIN-2013-060], Severo Ochoa Center of Excellence [SEV- 2012-0208].

Correspondence should be addressed to M Dierssen, Cellular & Systems Neurobiology, Systems Biology Program, Centre for Genomic Regulation (CRG), Dr. Aiguader 88, 08003 Barcelona, Spain, E-mail: mara.dierssen@crg.Eu

Cite as: eNeuro 2016; 10.1523/ENEURO.0103-16.2016

Alerts: Sign up at eneuro.org/alerts to receive customized email alerts when the fully formatted version of this article is published.

Accepted manuscripts are peer-reviewed but have not been through the copyediting, formatting, or proofreading process.

This is an open-access article distributed under the terms of the Creative Commons Attribution 4.0 International (http://creativecommons.org/licenses/by/4.0), which permits unrestricted use, distribution and reproduction in any medium provided that the original work is properly attributed.

²Universitat Pompeu Fabra (UPF), Barcelona, 08003, Dr. Aiguader 88, Spain

³Human Pharmacology and Clinical Neurosciences Research Group, Neurosciences Research Program, IMIM (Hospital Del Mar Medical Research Institute), Barcelona, 08003, Dr. Aiguader 88, Spain

⁴Comparative Bioinformatics, Bioinformatics and Genomics Program, Barcelona Institute of Science and Technology, Centre for Genomic Regulation (CRG), Barcelona, 08003, Dr . Aiguader 88, Spain

Department of Statistics and Operations Research, Universitat Politècnica De Catalunya/BARCELONATECH, Barcelona, Spain

⁶Centre for Research in Environmental Epidemiology (CREAL), Barcelona, 08003, Spain Dr. Aiguader 88

⁷Centro De Investigación Biomédica En Red De Epidemiología Y Salud Pública (CIBERESP), Spain

⁸Centro De Investigación Biomédica En Red De Enfermedades Raras (CIBERER), Spain

- 1 Title (50 word maximum)
- 2 Combined treatment with environmental enrichment and (-)-epigallocatechin-3-gallate
- 3 ameliorates learning deficits and hippocampal alterations in a mouse model of Down
- 4 syndrome.
- 5 Abbreviated title (50 character maximum)
- 6 Environmental enrichment and (-)-epigallocatechin-3-gallate as a therapy for DS
- 7 Author names and affiliations, including postal codes
- 8 Catuara-Solarz S^{1,3,7}, Espinosa-Carrasco J^{1,2,3}, Erb I^{2,3}, Langohr K^{7,8}, Gonzalez JR^{5,6},
- 9 Notredame C^{2, 3}, Dierssen M^{1,4, 7}
- 10 ¹Cellular & Systems Neurobiology, Systems Biology Program, The Barcelona Institute of
- 11 Science and Technology, Centre for Genomic Regulation (CRG), Dr. Aiguader 88, 08003
- 12 Barcelona, Spain
- 13 ²Comparative Bioinformatics, Bioinformatics and Genomics Program, Centre for Genomic
- 14 Regulation (CRG), Barcelona Institute of Science and Technology, Dr. Aiguader 88, 08003
- 15 Barcelona, Spain
- 16 ³Universitat Pompeu Fabra (UPF), Dr. Aiguader 88, 08003 Barcelona, Spain
- 17 ⁴Centro de Investigación Biomédica en Red de Enfermedades Raras (CIBERER), Spain
- 18 ⁵Centre for Research in Environmental Epidemiology (CREAL) Dr. Aiguader 88, 08003
- 19 Barcelona, Spain
- 20 ⁶Centro de Investigación Biomédica en Red de Epidemiología y Salud Pública (CIBERESP),
- 21 Spain

- 22 ⁷Human Pharmacology and Clinical Neurosciences Research Group, Neurosciences
- 23 Research Program, IMIM (Hospital del Mar Medical Research Institute), Dr. Aiguader 88,
- 24 08003 Barcelona, Spain
- 25 ⁸Department of Statistics and Operations Research, Universitat Politècnica de
- 26 Catalunya/BARCELONATECH, Barcelona, Spain
- 27 Corresponding author with complete address, including an email address and postal code
- 28 M Dierssen. Cellular & Systems Neurobiology, Systems Biology Program, Centre for
- 29 Genomic Regulation (CRG), Dr. Aiguader 88, 08003 Barcelona, Spain
- 30 mara.dierssen@crg.eu
- 31 Number of pages: 33
- 32 Number of figures: 5
- 33 Number of tables: 5
- 34 Number of words for:
- 35 Abstract: 136
- Introduction: 569
- 37 Discussion: 1097
- 38 Author contributions:
- 39 Authors contribution(s): SCS designed research, performed research, analyzed data, wrote
- 40 the paper; JEC, IE, KL, JRG analyzed data; CN supervised the PCA analysis, MD provided
- 41 financial support, designed research, wrote the paper.

43 Acknowledgements

This research was supported by DIUE of Generalitat de Catalunya (Grups consolidats SGR 44 45 2014/1125), Fondation Jérôme Lejeune (Paris, France), Spanish Ministry of Economy and 46 Finance (MINECO) grant numbers: SAF2013-49129-C2-1-R, BFU2011-28575 and 47 MTM2015-64465-C2-1-R CDTI ("Smartfoods"), the CIBER of Rare Diseases (ISCIII 48 initiative), and EU-Era Net Neuron PCIN-2013- 060. The CRG has received support as a 49 Severo Ochoa Center of Excellence SEV- 2012-0208. Silvina Catuara-Solarz received a FPI 50 doctoral fellowship from the Spanish Ministry of Economy and Finance (MINECO), 51 SAF2010-16427. We gratefully thank the students Carla Cuní-Lopez, Andrea Pérez and 52 María Alemany for their contribution in the data acquisition and technical assistance.

53 The authors declare no competing financial interests.

3

Abstract (max 250)

Intellectual disability in Down syndrome (DS) is accompanied by altered neuro-architecture, deficient synaptic plasticity and excitation-inhibition imbalance in critical brain regions for learning and memory. Recently we have demonstrated beneficial effects of a combined treatment with green tea extract containing (-)-epigallocatechin-3-gallate (EGCG) and cognitive stimulation in young adult DS individuals. Although we could reproduce the cognitive enhancing effects in mouse models, the underlying mechanisms of these beneficial effects are unknown. Here, we have explored the effects of a combined therapy with environmental enrichment (EE) and EGCG in Ts65Dn mouse model of DS at young age. Our results show that combined EE-EGCG treatment improved cortico-hippocampal dependent learning and memory. Cognitive improvements were accompanied by a rescue of CA1 dendritic spine density and a normalization of the proportion of excitatory and inhibitory synaptic markers in CA1 and DG.

Significance Statement (max 120)

Therapeutic methods for improving intellectual disability in Down syndrome (DS) are limited and their outcome remains unsatisfactory. Recently, we demonstrated that combined treatment with (-)-epigallocatechin-3-gallate (EGCG) and cognitive stimulation rescued cognitive deficits in DS individuals in a phase II clinical trial and also in middle age Ts65Dn mouse model of DS. Here, we show that EE-EGCG treatment improves cortico-hippocampal dependent learning and memory deficits in young trisomic mice, restores CA1 hippocampal dendritic spine density and mitigates disruptions in excitatory/inhibitory synaptic puncta in CA1 and DG.

Our results suggest that therapies with the capacity to simultaneously target several abnormal processes underlying intellectual disability and to efficiently act favoring physiological plasticity-enhancing interventions such as EE are optimal for disease-modifying interventions.

81 Introduction

82

83

84

85

86

87

88

89

90

91

92

93

94

95

96

97

98

99

100

101

102

103

104

105106

107

10,000 and 14 in 10,000 live births in European countries (Khoshnood et al., 2011) and the United States (Parker et al., 2010), respectively. It arises from the presence of an extra copy. or major portion of chromosome 21 (Hsa21), leading to a complex genetic imbalance (Antonarakis et al., 2004). Individuals with DS show moderate to severe cognitive impairment with an average intellectual quotient of 40-50 (de Sola et al., 2015), and 39.4% in the mild intellectual disability range of 50-70. The neuropsychological profile is characterized by marked hippocampal-dependent deficits particularly affecting spatial learning, memory and executive functions among other cognitive domains (Chapman and Hesketh, 2000; Nadel, 2003; Pennington et al., 2003). These cognitive deficits are associated with distinct neuro-architectural, synaptic, neurochemical alterations (for reviews Lott and Dierssen, 2010; Dierssen, 2012). At the cellular level, there is a reduction in dendritic number and complexity in cortical and hippocampal neurons, which affects synaptic connectivity (Becker et al., 1986). Furthermore, accumulating evidence suggest that DS pathophysiology is tightly associated with a disruption of the balance between the excitatory and inhibitory neuronal systems (Reynolds and Warner, 1988; Risser et al., 1997; Seidl et al., 2001; Bhattacharyya et al., 2009). These abnormalities are of particular importance since they are related to disruptions in neural plasticity, which is essential for cognition (Baroncelli et al., 2011). Several research groups have shown that it is possible to partially rescue DS phenotypes using non-pharmacological strategies such as postnatal handling or cognitive training by environmental enrichment (EE) that ameliorate behavioral and brain alterations in Ts65Dn mouse model of DS (Martínez-Cué et al., 2002; Dierssen, 2003; Begenisic et al., 2011; Chakrabarti et al., 2011; Golabek et al., 2011). It is widely accepted that EE is a cognitive enhancing intervention that promotes synaptic plasticity, adult neurogenesis and epigenetic modifications among other processes (for a review Sale et al., 2014). However, despite its beneficial effects, EE is not sufficient to promote long-lasting dendritic spine remodeling in

Down syndrome (DS) is the most common genetic form of intellectual disability with ~10 in

Ts65Dn mice (Dierssen, 2003) or significant developmental changes in DS children (Mahoney et al., 2004).

More recently, (-)-epigallocatechin-3-gallate (EGCG), the most abundant catechin found in green tea, with antioxidant and neuroprotective properties, has been shown to efficiently improve cognitive phenotypes in DS individuals and mouse models (De la Torre et al., 2014), ameliorate synaptic plasticity impairment in vitro (Xie et al., 2008) and restore excitatory/inhibitory (E/I) imbalance in Ts65Dn mice (Souchet et al., 2015). EGCG is a natural inhibitor of the kinase activity of Hsa-21 candidate gene Dyrk1A (Bain et al., 2003), whose overexpression is sufficient to induce cognitive and neuro-morphological alterations (Altafaj et al., 2001; Martinez de Lagran et al., 2012) and which is also modulated by EE (Golabek et al., 2011; Pons-Espinal et al., 2013). Recently, we showed that a combined treatment with EE and EGCG is more efficient than EE or EGCG alone to ameliorate ageassociated cognitive impairment of older Ts65Dn mice (Catuara-Solarz et al., 2015), suggesting a synergistic mechanism. Furthermore, we demonstrated that combined treatment with cognitive training and EGCG is more efficient than cognitive training alone to promote cognitive enhancement as well as neurophysiological recovery in young adults with DS in a phase II clinical trial (de la Torre et al., 2016). Thus, here we explored the effects of a combined EE-EGCG treatment on hippocampal cognitive, neuronal and synaptic alterations in young adult Ts65Dn mice.

Materials & methods

Animals

110

111

112

113

114

115

116

117

118

119

120

121

122

123

124

125126

127

128

129

130

131

132

133

Ts65Dn and wild type (WT) littermates were obtained through crossings of B6EiC3Sn a/A-Ts(17¹⁶)65Dn (Ts65Dn) females to B6C3F1/J males purchased from The Jackson Laboratory (Bar Harbor, ME) (RRID:IMSR_JAX:001924). The mouse colony was bred in the Animal Facilities of the Barcelona Biomedical Research Park (PRBB, Barcelona, Spain, EU). Mice were housed in standard or enriched conditions (see below) under a 12:12 hour light—

158

159

134 dark schedule (lights on at 8:00 a.m.) in controlled environmental conditions of humidity (60%) and temperature (22 °C ± 2 °C) with ad libitum access to food and water. Both the 135 136 Ts65Dn and euploid mice were genotyped by qPCR, in accordance with the Jackson 137 laboratories protocol (https://www.jax.org/research-and-faculty/tools/cytogenetic-and-down-138 syndrome-models-resource/protocols/cytogenic-qpcr-protocol). 139 Experiments were conducted using 1-2 months old female mice. We used females since 140 Ts65Dn males show high levels of stress in EE conditions that could mask the effect of the 141 treatment (Martínez-Cué et al., 2002). Although estrus cycle may be slightly delayed in 142 Ts65Dn mice, by the age of 2 months it is synchronized among all females (including 143 Ts65Dn and euploid mice) (Netzer et al., 2010). Thus, for the experiments carried out in this 144 study, it is unlikely that variations in estrogen levels between mice could influence behavior, 145 spine density or E/I balance. 146 All animal procedures met the guidelines of European Community Directive 2010/63/EU and 147 the local guidelines (Real Decreto 53/2013) and were approved by the Local Ethics 148 Committee (Comité Ético de Experimentación Animal del PRBB [CEEA-PRBB]; procedure 149 numbers MDS-08-1060P2 and MDS-14-1611). 150 Environmental enrichment and (-)-epigallocatechin-3-gallate (EGCG) 151 Ts65Dn and WT 1-2 months old female mice were assigned to either control conditions or a 152 combination of EE and green tea extracts containing 45% EGCG using a simple 153 randomization. Mice received the treatments for 30 days based on previous studies (De la Torre et al., 2014; Catuara-Solarz et al., 2015). In the control conditions animals were reared 154 155 in conventional cages (20 × 12 × 12 cm height, Plexiglas cage) in groups of 2-3 animals. EE housing consisted of spacious (55 × 80 × 50 cm height) Plexiglas cages with toys, small 156

houses, tunnels, and platforms of different shapes, sizes, colors and textures. Wheels were

not introduced in the cages in order to avoid the effect of physical exercise. The

arrangement was changed every 2 days to keep novelty conditions. To stimulate social

interactions, 6–8 mice were housed in each cage. Green tea extract containing 45% of EGCG was administered in drinking water (EGCG dosage: 0.326 mg/ml, 0.65 mg per day; 30 mg/Kg per day) by preparing fresh EGCG solution every 2 days from a green tea leaf extract (Mega Green Tea Extract, Decaffeinated, Life Extension®, Florida, USA; EGCG content of 326.25 mg per capsule).

Morris water maze (MWM)

160

161162

163

164

165

166

167

168

169

170

171

172

173

174

175

176

177

178

179

180

181

182

183

184 185

186

The Morris water maze was performed according to a previously described method (Catuara-Solarz et al., 2015). Briefly, mice were trained in a water maze (pool: 1.70 m diameter, platform: 12 cm diameter) during five learning sessions (four acquisition trials per session and 1 session per day). 24 h after the last acquisition session, mice underwent one probe/removal session (reference memory trial) in which the platform was removed, followed by one cued session. Starting the following day, 3 reversal sessions (four trials per session) were conducted where the platform position was changed 180° to test cognitive flexibility as a measure of executive function. In every session, mice randomly entered the pool from four different positions and were allowed to search the platform for 60 s. The same experimenter performed all the MWM procedures being blind for mice genotype. Mice were video-tracked during the test and their latency to reach the platform, total distance swum, time spent in periphery and swimming speed were recorded using SMART software (Panlab, Spain, RRID:SCR 002852). Subsequently, data were computed with a software previously developed by our lab (Jtracks; Arqué et al., 2008) in order to obtain other measurements to quantify the most efficient and direct trajectory from the location of mice to the platform, such as the Gallagher index (average distance from each mouse to the center of the platform), the Gallagher distance (accumulated distance from each mouse to the center of the platform) and the Whishaw index (percentage of path inside the optimal corridor connecting release site and goal) (Whishaw and Jarrard, 1996). Mice that did not reach the platform in less than 30 s in the cue session were considered unsuitable for the test and were subtracted from the analysis. One over-performing mouse from the EE-EGCG treated TS group was removed

from the analysis. The estimate of the number of mice required (n = 10) was based on the expected difference between the experimental groups, deriving from previous data obtained in our laboratory (n mice: WT=11; TS=8; WT-EE-EGCG=12; TS-EE-EGCG=8).

Novel object recognition test

The novel object recognition test was performed as an adaptation from the protocols described in Leger et al. (2013). The procedure was conducted in a V-maze apparatus (walls height = 27 cm, arm length = 30 cm and arm width = 6 cm). First, mice were subjected to a 5 min habituation session during which mice were allowed to explore the maze without any objects. The following day mice went through a 10 min familiarization session where two identical objects were situated at the end of each arm attached to the wall and the floor with adhesive tape. After a 60 min inter-trial interval, the recognition test session was conducted consisting on a 5 min trial in which one of the objects used at familiarization was substituted by a new object. Recognition of the new object was assessed by calculating the discrimination index (DI) by the following formula DI = (novel object exploration time/total exploration time) – (familiar object exploration time/total exploration time) – (familiar object exploration time/total exploration time) X 100. Exploratory behavior was defined as the mouse directing its head or sniffing towards the object at a distance of approximately 1-2 cm. The estimate of the sample size was based on previous data obtained in our laboratory (n mice: WT = 8; TS = 7; WT-EE-EGCG = 7; TS-EE-EGCG = 7).

Golgi neuronal staining and dendritic spines imaging

To avoid confounding effects, these experiments were performed with mice that did not undergo behavioral assessment. Golgi staining was performed according to manufacturer instructions (SuperGolgi Kit – Bioenno Tech Cat# 003010, RRID:AB_2620135). Mice were sacrificed with CO₂ and perfused intracardially with phosphate buffered saline (PBS) 0.01 M

213

214

215

216

217

218

219

220

221

222

223

224

225

226

227228

229

230

231

232

233

234

235

236

237

238

239

followed by chilled 4% paraformaldehyde (PFA). Brains were removed from the skull and postfixed in the same fixative at 4°C overnight. Brain hemispheres were immersed freshly into impregnation solution during 9 days. When impregnation was ready the tissue blocks were rinsed with distilled water and transferred into post-impregnation buffer during 4-5 days at room temperature (RT) in the dark. The solution was renewed after one day of immersion. After that, brains were cut with a vibratome (VT1000S; Leica Microsystems) in sections of 150 µm and were kept in collection and mounting buffer. Sections were mounted on adhesive microscope slides and gentle pressure was applied with filter paper over the sections to enhance the adhesion. Slides were washed in PBS 0.01 M - 0.3%Triton X-100 for 20-30 min and then placed in the staining solution for 20 min in a closed dark jar. After that, slides were moved to the post-staining buffer for 20 min in a dark area and then washed in PBS 0.01 M - 0.3% Triton X-100 for 15 min. Slides were dried in a closed jar at RT during 1 day. Finally, sections were dehydrated in 100% ethanol for 5-10 min and cleared in xylene for another 10 min. Slides were covered with coverslips using mounting medium and were kept at RT in a dark area. Images were acquired from outer molecular layer secondary apical dendrites of granule neurons (located at 40 - 90 µm from the neuronal soma) of the dentate gyrus (DG) and secondary apical dendrites from pyramidal neurons from the Cornu Ammonis 1 (CA1) (located at 50 - 100 µm from the neuronal soma). These hippocampal regions were selected since they play a critical role in the process and storage of spatial information (Tsien et al., 1996; Deng et al., 2010). To do so, we used an Olympus BX51 microscope with 100X objective and the Neurolucida software (11.03.1, MBF Bioscience, Williston, VT USA, RRID:SCR 001775). Quantification of dendritic spine density was performed on 20 µm dendritic segment length using the NIH ImageJ software 1.46a version and multipoint plugin. The criterion to define dendritic spines was the identification of tridimensional protrusions emerging from the dendritic shaft that could be visualized across the Z planes. For this experiment we used 3 brain slices per mouse of the dorsal hippocampus (Bregma: 1.82-1.94, Paxinos mouse brain atlas) of 5-6 mice per experimental group. From each brain slice, 2-3 dendrites from each hippocampal subregion were imaged

243

244

245

246

247

248

249

250

251

252

253

254

255

256

257

258

259

260

261

262

263

264

265

266

(number of dendrites in the DG: WT = 46; TS = 42; WT EE-EGCG = 48; TS EE-EGCG = 42; number of dendrites in CA1: WT = 38; TS = 32; WT EE-EGCG = 31; TS EE-EGCG = 39).

Immunohistochemical labeling of excitatory and inhibitory synaptic vesicle proteins

Synaptic modifications due to genotype and treatment were addressed by performing immunohistochemical labeling for vesicular glutamate transporter 1 (VGLUT1) and vesicular GABA transporter (VGAT). Animals were exposed to CO₂ and afterwards perfused intracardially with PBS 0.01 M, pH 7.5, followed by 4% PFA. Brains were removed and kept at 4°C in 4% PFA ON and then were transferred to a solution of 30% sucrose in PBS for 2 days. Series of coronal sections (40 µm) were obtained using a vibratome (VT1000S; Leica Microsystems) and stored at -20°C in a cryoprotector solution (30% ethylene glycol, 30% glycerol, 40% PBS). Free-floating brain sections were permeabilized with 0.3% Triton X-100 in PBS for 30 min at RT and then incubated for 20 min with Glycine (50 mM) in PBS - 0.3% Triton X-100. After that slices are washed for 15 min with PBS- 0.3 % Triton X-100 and blocked with 5% normal goat serum (NGS)/PBS-0.3% Triton X-100 for 1h at RT. Subsequently, sections were incubated overnight at 4°C with the primary antibodies mouse anti-vesicular glutamate transporter 1 (VGLUT1) monoclonal antibody (1:150; Cat. No. 135 511, Synaptic Systems, RRID: AB 887879) and guinea pig anti-vesicular GABA transporter (VGAT) polyclonal antibody (1:200; cytoplasmic domain, Synaptic Systems Cat. No. 131004, RRID:AB 887873) in 0.1% Triton X-100/2.5% NGS in PBS. After that, slices were washed with PBS-0.3% Triton X-100 and incubated with secondary antibodies Alexa Fluor 488 goat anti-mouse Cat. No. A11001, RRID:AB 2534069, and Alexa Fluor 555 anti-Guinea Pig Cat. No. A-21435, RRID:AB 2535856 (1:1000)/ 0.1% Triton X-100/2.5% NGS in PBS for 2 h at RT, protected from light. Finally, sections were washed with PBS-0.3% Triton X-100, nuclei were stained with Hoescht (1:1000) in PBS for 10 min and tissues were mounted on glass slides with Mowiol reagent. Images were acquired from DG and CA1 hippocampal regions using a confocal microscope with a 63X objective (TCS SP5, Leica Microsystems) and the LAS AF software. For each region, all pictures were captured with identical confocal settings

for laser power, gain, and offset levels. Images were imported into NIH ImageJ software v.1.46a, converted into binary data and thresholded in order to achieve maximum number of individual puncta without causing puncta fusion. The same threshold was applied to all the images in order to outline puncta number, size and % of area occupied by puncta, using the "analyze particle" plugin. For this experiment we used 2 brain slices of the dorsal hippocampus (Bregma: 1.82-1.94, Paxinos mouse brain atlas) of 4 mice per experimental group. From each brain slice 4-5 images were acquired per hippocampal subregion.

Statistical analysis

Behavioral experiments

Morris water maze

Single-variate analysis. Differences among experimental groups over time were tested using a single-variate analysis for selected learning-related parameters (latency to reach the platform, Gallagher index and % of time spent in the periphery) using one-way repeated measures ANOVA. To avoid ceiling effect of mice unable to solve the task, the variable "latency" was considered right-censored when reaching the maximum allowed time (60 s; Vock et al., 2012) using a Tobit model implemented in the censReg package from The R Foundation for Statistical Computing (RRID:SCR_001905), version 3.2.1 (Henningsen, 2011). Multiple comparisons for parametric models were used to address post-hoc comparisons using the multest R package and the glht function (Hand and Taylor, 1987; Dickhaus, 2012). To control the false discovery rate (FDR) due to multiple post-hoc comparisons, the Benjamini-Hochberg method was used (Benjamini and Hochberg, 1995).

Principal Component Analysis (PCA). We used PCA to identify the linear combinations of the original variables (latency to reach the platform, percentage of time spent in target quadrant, percentage of time spent in the periphery, Whishaw index, Gallagher index, distance traveled, and speed) that explain the maximum amount of experimental variability. More

precisely, our application of the method aims primarily at two kinds of variability: the variation among experimental groups for a given learning session and the variation of a given group across learning sessions. For this, we implemented the same procedure as described in Catuara-Solarz (2015). Briefly, a PCA for the acquisition sessions was performed on 20 observations of 7 variables. Here the observations correspond to the 4 experimental groups on the 5 learning sessions, and the variables are the experimental parameters described above. The resulting 20 x 7 data matrix contains the medians of the measured variables for each group during each session (the 4 trials per mouse of each learning session were averaged). As variables are measured in different units, they were scaled to unit variance to enable a combined analysis. The result of the described PCA approximates a decomposition of what is commonly called between-group variance. A third kind of variability coming from individuals within a group for a given session can also be quantified. For this, 195 supplementary points that correspond to the 39 individuals appearing five times each were projected. The R-package FactoMineR was used (Lê et al., 2008). Separately, a similar PCA was done for the three reversal sessions.

Our analysis can be considered a discriminant analysis in the sense that the PCA is performed for groups and individuals are projected only after the PCA is performed. However, the fact that we use group medians instead of the commonly applied group means weighted by group sizes leads to two differences: first, between-group variance is defined as variance between group medians; second, the overall barycentre no longer coincides with the group barycentre (our origin) and thus the total variance obtained by summing squared distances of all individuals from the origin as applied in (Catuara-Solarz 2015) overestimates the true variance by a small amount (i.e. by the squared distance of the barycentre from the origin). To comply with the original definition (see Greenacre, 2010 chapter 11) of betweengroup variance when decomposing total variance, the overall barycentre instead of the origin can be used as the reference point and weighted group means obtained from the supplementary points can be used to calculate the between-group variance instead. We

319 found that the difference between both approaches is on the order of a few percent points 320 only. 321 To validate the stability of the PCA, we used a jackknifing procedure that consists in the 322 following: each individual is subtracted from the analysis and the resulting modified group 323 median is used to perform a new PCA. The angle between the new PC 1 and 2 with respect 324 to the original principal axes is computed. The procedure showed that both axes remain very 325 stable, with PC1 attaining maximum angles around one degree, suggesting a minor 326 influence of the small number of experimental groups on the outcome of the analysis (data 327 not shown). 328 Density plots were obtained using the statdensity 2d function from the ggplot2 R package 329 (Wickham, 2009) RRID:SCR 014601 with the parameters: n = 100, h = 4, and bins = 6. In 330 order to assess statistical significance of group separation, we randomly re-assigned 331 individuals to experimental groups to perform a permutation test (Sham and Purcell, 2014) 332 where original numbers of individuals in each group were kept. For this, learning differences 333 were evaluated using a t-statistic involving PC1 pairwise group comparisons based on 334 supplementary points. All pairwise comparisons were determined at each permutation. The 335 number of randomized PCAs was 10,000. Finally, to evaluate the change in within-group 336 variances before and after learning, we averaged squared distances of a group's 337 supplementary points from their barycentre using coordinates from all seven principal axes. 338 Novel object recognition 339 Differences in the discrimination index among experimental groups were tested using a one-340 way ANOVA. Tukey multiple comparisons for parametric models were used to address posthoc comparisons using the multest R package and the glht function (Hand and Taylor, 1987; 341 342 Dickhaus, 2012). To control the false discovery rate (FDR) due to multiple post-hoc 343 comparisons, the Benjamini-Hochberg method was used (Benjamini and Hochberg, 1995).

345	Dendritic spine density and excitatory (VGLUT1) and inhibitory (VGAT) synaptic
346	puncta
347	For the analysis of the differences among the experimental groups in dendritic spine
348	densities and number, size and % of area occupied by synaptic puncta of VGLUT1 and
349	VGAT, we used linear mixed models, which included the experimental group as a factor and
350	mouse as a random effect to account for the repeated measures per mouse. The F-test was
351	used to evaluate the global hypothesis that there was no association between the response
352	variables and the groups. Whenever this hypothesis was rejected, post-hoc tests for the
353	following contrasts of interest were applied: WT vs. TS; TS – TS EE-EGCG and WT vs. WT
354	EE-EGCG. The analyses were performed using R packages nlme (Pinheiro et al., 2016) and
355	multcomp (Hothorn et al., 2008) for the fit of the linear mixed models and the multiple tests
356	respectively. Statistical significance was set at 0.05. The significance levels for the 3
357	contrasts of interest were adjusted in order to guarantee a family-wise error rate of 0.05.
358	Results
359	Effects of EE-EGCG treatment on cortico-hippocampal-dependent learning and
360	memory impairment in Ts65Dn mice
361	To evaluate the effect of EE-EGCG treatment we compared the behavioral performance o
362	WT and Ts65Dn mice treated with EE-EGCG with their untreated counterparts in the MWM
363	During the acquisition sessions there were statistical differences among all groups in escape
364	latency, distance to the target, as shown by both the Gallagher index (mean distance to the
365	platform) and the Gallagher (accumulated) distance to the platform and thigmotaction
366	behavior, the percentage of time spent close to the periphery of the pool (Table 1).
367	We detected learning defects in Ts65Dn mice compared to WT (Fig. 1A) as shown by the
	higher escape latency across sessions (Fig. 1B. Table 1) increased Gallagher distance and
368	

369 index (Fig. 1A and C, and Table 1) and the typical increase in thigmotactic behavior (Fig. 1A 370 and D, Table 1). 371 EE-EGCG treated Ts65Dn mice showed improved learning performance during the 372 acquisition sessions (Fig. 1A). In comparison to untreated Ts65Dn, EE-EGCG treated 373 Ts65Dn mice presented significantly reduced escape latency (Fig. 1B, Table 1) and 374 Gallagher distance and index (Fig. 1 A and C, Table 1) but no statistical differences in thigmotactic behavior (Fig. 1 A and D, Table 1). Conversely, EE-EGCG treated WT mice did 375 376 not show differences compared to untreated WT. 377 There were differences in swimming speed among the groups and specifically Ts65Dn 378 presented lower swimming speed than WT (data not shown, Table 1). However, EE-EGCG 379 did not promote significant changes in swimming speed, neither in Ts65Dn nor in WT with 380 respect to the untreated condition (data not shown, Table1). This suggests that the learning 381 differences in EE-EGCG treated Ts65Dn mice are not mediated by changes in swimming 382 speed. 383 To assess reference memory, a probe trial (removal session) was performed 24 h after the 384 last acquisition day. In this session there were no differences among all the groups in the 385 percentage of time spent in the target quadrant probably due to the high variability of the 386 data (data not shown). However, the latency to the first entry to the platform area and the 387 Gallagher distance, which is a more precise performance measure (Maei et al., 2009), 388 showed significant differences among experimental groups (Fig.1A, E and F, Table 1). Post-389 hoc analysis demonstrated higher values of Ts65Dn mice in the Gallagher distance and the 390 latency to the first entry compared to WT mice (Fig. 1A, E and F, Table 1) indicating poorer 391 reference memory. The mean difference in these parameters between EE-EGCG treated and untreated Ts65Dn mice was fairly large; however, it did not reach statistical significance 392 393 possibly due to high variability of the data (Fig. 1A, E and F, Table 1).

In the reversal sessions we detected statistical differences among the experimental groups in escape latency, Gallagher distance and index, and thigmotaxis (Table 1). While untreated WT mice efficiently shifted their search to the new platform position (Fig. 1A), Ts65Dn presented increased escape latency (Fig. 1G, Table 1), increased Gallagher distance and index (Fig. 1A and H, Table 1) and increased thigmotaxis across the 3 reversal learning sessions (Fig. 1A and I, Table 1), as compared to WT. During reversal, there was no significant reduction in thigmotaxis suggesting that this variable was not associated to reversal learning.

EE-EGCG treated Ts65Dn mice showed a fairly large although not statistically significant reduction in the latency to reach the new platform position as compared to untreated Ts65Dn mice (Fig. 1A and G, Table 1). There were no significant differences between EE-EGCG treated and untreated Ts65Dn mice in either Gallagher distance or index (1A and H, Table 1) or thigmotaxis (Fig. 1A and I, Table 1). EE-EGCG treated and untreated WT mice showed no significant differences in the latency to reach the new platform position, the Gallagher distance or index or thigmotaxis. During the reversal sessions there were no statistical differences on swimming speed among the experimental groups (not shown, Table 1).

Multidimensional analysis of learning using PCA

PCA allowed to place the experimental groups in a low-dimensional coordinate system built from variables taken during the MWM experiment. A group's progression along the acquisition sessions becomes apparent in its resulting five-day trajectory (Fig. 2A). We obtained a first principal component (PC1) that explained 84% of the between-group variance and was mainly composed of learning-related variables (i.e. escape latency, Gallagher index, % of time spent in periphery, Whishaw index, distance travelled, % time spent in target quadrant; Figs. 2B and C). Swimming speed also contributed to PC1, but to a lesser extent. Efficient learning behaviors (short distances to target, low escape latencies, high percentages of time in the target quadrant, etc.) correspond to large values in PC1 (Fig.

421 422

423

424

425

426

427

428

429

430

431

432

433

434

435

436

437

438

439

440

441

442

443

444

445

2B) and thus PC1 can be interpreted as a quantification of learning. In contrast, the second principal component (PC2) explained 11% of between-group variance and was mainly composed of swimming speed (Figs. 2B and D). This component of speed is unrelated to learning since PC2 is orthogonal to the learning-related PC1. It thus seems to reflect motor performance rather than determination to reach the target quickly. Swimming speed is thus decomposed in a learning-dependent component (PC1) and a learning-independent component (PC2). Learning-related variables contributed to a much lesser extent to PC2. Since a group trajectory represents a group's overall learning through its progression along PC1, the trajectory representation allows for effective comparisons between group performances. Untreated Ts65Dn mice showed a trajectory reaching a maximum value of PC1 that corresponds to initial PC1 values of the untreated WT trajectory, revealing poor learning. On the other hand, the EE-EGCG treated Ts65Dn trajectory attained more advanced maximum values of PC1. Additionally, we determined individual variation within the groups by mapping the position of each individual on each acquisition day to the PCA plot. As shown in the density plots of sessions 1 and 5 in Fig. 2E, there is substantial individual variation across learning sessions in all the experimental groups. In fact, overall group differences explain less than half of the total variance. Within-group variance however differs between experimental groups. While WT generally show higher variability than Ts65Dn, the treatment roughly doubles variance for both genotypes in the first learning session. Interestingly, learning increases variability in all groups. This effect is stronger for untreated groups, so that treated and untreated groups show similar variability in the last learning session. We summarize within-group variances in the first and last acquisition sessions in Table 2. To assess the statistical significance of differences in learning we performed a permutation test involving a t statistic based on PC1. Untreated Ts65Dn mice presented significantly

lower PC1 values in comparison to WT mice in the first learning session (Fig. 2F, Table 3).

446	EE-EGCG treated Ts65Dn presented higher PC1 than untreated Ts65Dn (Fig. 2F, Table 3)
447	at this stage that could be associated with procedural learning and were not significantly
448	different from untreated WT (Fig. 2F, Table 3). At the end of the learning period (session 5)
449	untreated Ts65Dn mice still presented significantly lower PC1 values in comparison to WT
450	mice (Fig. 2F, Table 3). EE-EGCG treated Ts65Dn exhibited higher PC1 than untreated
451	Ts65Dn, although they showed significantly lower PC1 values than untreated WT (Fig. 2F,
452	Table 3). On the other hand, EE-EGCG treatment did not significantly change learning
453	outcomes of WT mice either in the first or in the last session.
454	Similarly, group trajectories comprising three time points each were obtained for the reversal
455	sessions (Fig. 3A). Here, PC1 explained 84% of the between-group variance and, as in the
456	acquisition sessions, was dominated by learning-related variables (Fig. 3B and C). PC2,
457	which explained 12% of the between-group variance, showed again a strong contribution of
458	swimming speed. The main contribution here, however, turned out to be from thigmotaxis
459	(Fig. 3B and D). Interestingly, these two variables fall on a line separating the groups along
460	an efficiency gradient from strong thigmotaxis and low speed to no thigmotaxis and high
461	speed following the ordering TS, TS-EE-EGCG, WT and WT-EE-EGCG (Fig. 3A and B).
400	
462	Again, there was an increased within-group variability associated with the learning process
463	in all groups (Fig. 3E and Table 2).
464	According to the permutation tests, untreated Ts65Dn mice showed significantly lower PC1
465	than untreated WT mice (Fig. 3F, Table 2). EE-EGCG treated Ts65Dn presented
466	significantly higher PC1 than untreated Ts65Dn, although they still showed significantly
467	lower PC1 than WT (Fig. 3F, Table 2). In WT mice EE-EGCG treatment did not modify
468	cognitive flexibility outcomes neither in the first nor the last session.

Effects of EE-EGCG treatment on recognition deficits in Ts65Dn mice

470	In order to assess the impact of the treatment on a less stressful learning task we conducted
471	a novel object recognition test. The performance of this test depends on the functionality of
472	the entorhinal and perirhinal cortices and the hippocampus (Brown & Aggleton 2001).
473	In this test Ts65Dn mice showed no deficit in their discrimination index (DI) in comparison to
474	WT mice, although a slight tendency to impairment was detected (p=0.08, Fig. 4, Table 4).
475	EE-EGCG treated Ts65Dn mice presented an increase in their DI with respect to their
476	untreated counterparts (Fig. 4, Table 4) and scored at similar levels to WT mice (Fig. 4 Table
477	4). Conversely, EE-EGCG treated WT mice showed a poorer performance than untreated
478	WT mice (Fig. 4 Table 4).
479	
480	Effects of EE-EGCG treatment on dendritic spine density in Ts65Dn hippocampus
481	Ts65Dn mice showed a significant reduction of dendritic spine density in the CA1 (Fig. 5A,
482	Table 5) and DG (Fig. 5B, Table 5) hippocampal subregions. EE-EGCG treated Ts65Dn did
483	not show statistically significant differences in DG dendritic spine density neither with
484	Ts65Dn nor with WT mice (Fig. 5B). Conversely, EE-EGCG treated Ts65Dn mice presented
485	an increased dendritic spine density in CA1 in comparison to untreated Ts65Dn (Fig. 5A,
486	Table 5). On the other hand, EE-EGCG treated WT mice showed reduced CA1 dendrition
487	spine density in comparison to untreated WT (Fig. 5A, Table 5).
488	Effects of EE-EGCG treatment on hippocampal excitatory and inhibitory synaptic
489	puncta in Ts65Dn
490	In DG, Ts65Dn mice showed increased VGLUT1 puncta density (data not shown, Table 6) of
491	reduced size (data not shown, Table 6), and no differences in the number or size of VGAT
492	puncta as compared to WT. This resulted in an increased VGLUT1/VGAT density ratio (Fig.
493	6A, Table 6). Since the increase in the number of VGLUT1 puncta was compensated by a
494	reduction in size, Ts65Dn showed no difference in the VGLUT1/VGAT percentage of area
495	occupied as compared to WT (Fig. 6B. Table 6)

496 In CA1 Ts65Dn mice also showed significantly increased density of VGLUT1 puncta of reduced size compared to WT (data not shown, Table 6). As in DG, Ts65Dn presented no 497 498 differences in VGAT density puncta in CA1 but in this region, VGAT puncta were enlarged 499 (data not shown, Table 6). This resulted in an increased ratio of VGLUT1/VGAT puncta density (Fig. 6C, Table 6), and a reduced VGLUT1/VGAT percentage of area occupied (Fig. 500 501 6D, Table 6). 502 Compared to untreated conditions, EE-EGCG treated Ts65Dn exhibited a significant 503 reduction in the density of VGLUT1 puncta in DG (data not shown, Table 6) but not in CA1. 504 VGLUT1 puncta were significantly enlarged in DG (data not shown, Table 6) but not in CA1. 505 There were no significant differences in VGAT puncta number or size between EE-EGCG 506 and untreated Ts65Dn in DG or CA1. As a result, EE-EGCG treated Ts65Dn mice showed a 507 reduction in the ratio of VGLUT1/VGAT density both in DG (Fig. 6A Table 6) and in CA1 508 (Fig. 6C, Table 6) leading to values that were similar to those of WT. 509 On the other hand, EE-EGCG treated WT mice also showed a trend towards an 510 enlargement of VGAT puncta size in CA1 (data not shown, Table 6) leading to a decreased 511 VGLUT1/VGAT percentage of area occupied (Fig. 6D, Table 6) in comparison to untreated 512 WT mice. 513 Discussion 514 In the present study, combined EE-EGCG treatment significantly increased spine density in 515 CA1, normalized excitatory and inhibitory synaptic markers in CA1 and DG and improved 516 performance in a cortico-hippocampal dependent learning task in young Ts65Dn mice. 517 In line with previous studies, we detected poor learning strategies and hippocampal-518 dependent learning and memory performance in the MWM in young Ts65Dn mice 519 (Escorihuela et al., 1995; Reeves et al., 1995). In Ts65Dn mice, but not in WT, EE-EGCG

treatment improved performance in the MWM reducing escape latency and Gallagher index

522

523

524

525526

527

528

529

530

531

532

533

534

535

536

537

538

539

540

541 542

543

544

545

546

and distance during the learning sessions. Principal component analysis confirmed that untreated Ts65Dn showed inefficient learning progress over acquisition sessions, reaching maximum values of PC1, a global learning variable, similar to initial WT values. EE-EGCG treated Ts65Dn improved on global learning measures. They reached more advanced maximum PC1 values than untreated Ts65Dn, suggesting a modification in learning related behavior as previously reported in middle age Ts65Dn mice (Catuara-Solarz et al., 2015). Ts65Dn mice also exhibited poor reference memory, as indicated by a significantly increased Gallagher index and distance and latency to the first entry to the platform area in the probe trial. However, no genotype effects were detected in other variables such as time spent in the target quadrant or latency to first entry to target area probably due to the high variability of the data. Additionally, Ts65Dn presented a deficit in cognitive flexibility, as shown by the inefficient performance during the reversal sessions (executive function). Single-variate analysis of different parameters between EE-EGCG treated and untreated Ts65Dn mice did not reach statistical significance at reference memory and reversal sessions. However, a significant enhancement in cognitive flexibility was shown by multivariate analysis of the reversal sessions. In middle age Ts65Dn mice, EE-EGCG treatment improved learning and reference memory, but not cognitive flexibility (Catuara-Solarz et al., 2015). This suggests that EE-EGCG treatment effects are age and cognitive domain-dependent possibly due to differential effects on different underlying brain regions and functions at different ages. EE-EGCG treated WT mice did not show significant differences possibly due to ceiling effect. The MWM is a learning paradigm that is based on the stressful and aversive stimuli of the water pool which triggers increases in plasma corticosterone leading to a motivational state in the mice to learn the spatial configuration of the cues to escape (Harrison et al., 2009).

Previous studies have shown that EGCG exerts an anxiolytic effect on different behavioral

anxiety tests such as the forced swimming test, elevated plus maze, passive avoidance test and the tail suspension test (for a review Dias et al., 2012). It could be thus speculated that the potential anxiolytic effects of EGCG would contribute to the learning improvement we found in the MWM. However, a number of facts suggest that the learning improvements found in treated Ts65Dn mice are not mainly contributed by the anxiolytic effect of EGCG. Ts65Dn have reduced levels of anxiety-like behavior in the elevated plus maze (Coussons-Read 1996, Demas 1996, Escorihuela 1998, Shichiri 2011), suggesting that the learning deficits shown by Ts65Dn in the MWM are not associated to anxiety and thus a potential anxiolytic effect of EGCG would not eventually lead to significant learning improvement. Additionally, in the case of a potential MWM improvement associated to the anxiolytic effect of EGCG we should be able to observe it in the control group as it is also subjected to the same anxiogenic scenario. However in our study the WT group is not benefitted by the combined EE-EGCG treatment.

Even so, we also addressed the effects of the combined EE-EGCG treatment in a less stressful learning test such as the novel object recognition test. The performance of this test depends on the functionality of the entorhinal and perirhinal cortices and on the hippocampus (Brown and Aggleton, 2001; Brown et al., 2010). In this test, trisomic mice presented no significant deficit in their discrimination index (DI) in comparison to WT mice, similar to some previous reports (Hyde and Crnic, 2002), although a slight tendency to impairment was detected which is in line with data from Fernandez et al (2007). EE-EGCG treated Ts65Dn mice presented an improvement in their DI with respect to their untreated counterparts and scored at similar levels to WT mice. On the other hand EE-EGCG treated WT mice showed a poorer performance than untreated WT mice, suggesting a possible deleterious effect of EGCG.

Along with learning improvement, EE-EGCG treated mice also showed significant neuro-morphological changes in the hippocampus. Consistently with previous reports in DS (Ferrer

575

576

577

578

579

580

581

582

583

584

585

586

587

588

589

590

591

592

593 594

595

596 597

598

599

600

and Gullotta, 1990) and Ts65Dn (Belichenko et al., 2004), we observed a reduction in dendritic spine density in outer molecular layer dendrites from granule cells of the DG, and in apical dendrites of pyramidal neurons of CA1 in Ts65Dn mice. Combined treatment with EE-EGCG partially rescued the dendritic spine density deficit in CA1, but not in the DG of Ts65Dn. A reduction of Dvrk1A kinase activity (Bain et al., 2003; Golabek et al., 2011; Pons-Espinal et al., 2013), but also other signaling pathways that are modified by both EE and EGCG, such as increased CREB and Akt phosphorylation (Jia et al., 2013; Ramírez-Rodríguez et al., 2014; Ortiz-López et al., 2016), or increases in BDNF expression (Young et al., 1999; Li et al., 2009a, 2009b), could contribute to these neuroplasticity changes. We also explored the effects of EE-EGCG treatment on excitation-inhibition balance, using excitatory (VGLUT1) and inhibitory (VGAT) synaptic vesicle markers. In Ts65Dn DG, VGLUT1 puncta were more abundant but smaller, with no changes in the percentage of area occupied, while VGAT puncta showed no differences as compared to WT littermates. In CA1, Ts65Dn showed the same phenotype, being VGLUT1 puncta more abundant and smaller, however in this region VGAT puncta were enlarged, leading to an increased VGLUT1/VGAT ratio, but a reduction of VGLUT1/VGAT percentage of area occupied. The fact that in both DG and CA1 VGLUT1 puncta were more abundant and smaller in Ts65Dn could affect the probability or efficiency in neurotransmitter release (Harris and Sultan, 1995; Bozdagi et al., 2000; Antonova et al., 2001; Bamji et al., 2006; Bourne et al., 2013) and could also be related to the previously reported enhanced GABAA and GABAB evoked inhibitory postsynaptic currents in DG of 3-4 months old male mice (Kleschevnikov et al., 2012) and increased GABA release in the hippocampus of male and female adult mice (Begenisic et al., 2011). Consistent with our results, previous work showed no changes in density of VGAT puncta nor in density of inhibitory synapses using electron microscopy in the DG of 3 months old male mice, although apposition length of symmetric (inhibitory) synapses was larger (Belichenko et al., 2009). Additionally, Kleschevnikov et al. (2012),

found no differences in GAD67 optical density in DG, with only a trend towards reduction in

602

603

604

605

606

607

608

609

610

611

612

613

614

615

616

617

618

619

620

621

622

623

624

625

626

GAD67 in the outer molecular layer of 3-4 months old male mice. A recent study using western blots showed a reduction in the hippocampal expression of VGLUT1 and a not statistical difference in VGAT (Souchet et al., 2015). Conversely, others have shown an increase in the percentage of area occupied by VGAT puncta and VGAT/Gephyrin puncta in DG of 4.5-5.5 months old male mice (Martinez-Cue et al., 2013). Differences in experimental methods, hippocampal subregions, age or gender could account for these divergent results. On the other hand, very little is known about how E/I is affected across different brain regions or ages in Ts65Dn. Possibly, the E/I imbalance could arise from alterations in excitation, inhibition, or both and may be continuously changing as a result of synaptic plasticity, leading to region-specific dysfunction (Bartley et al., 2015). Interestingly, EE-EGCG treated Ts65Dn mice showed normal density and size of VGLUT1 puncta, and as a consequence, the balance of excitatory and inhibitory puncta in DG and in CA1 was also in the normal ranges. The fact that the treatment restores the density and size of VGLUT1 puncta is consistent with the treatment effect on the density of dendritic spines. Excitatory synapses are comprised by a presynaptic terminal with abundant synaptic vesicles containing glutamate, in association with dendritic spine heads acting as a postsynaptic element. Thus, our results suggest that combined treatment with EE-EGCG may increase excitatory synaptic connections. These results are also consistent with the outcome of a recent phase II clinical trial with DS individuals where a therapy combining cognitive training and EGCG normalized neuronal networks functionality as measured by fMRI and cortical excitability by TMS (de la Torre et al., 2016). Conversely, in WT mice EE-EGCG treatment reduced spine density in CA1, but not in the DG, and led to excitatory/inhibitory imbalance in CA1, without significant changes in the DG. This deleterious effect could be explained by an over-inhibition of Dyrk1A kinase activity in WT conditions, since it has been shown that DYRK1A haploinsufficiency is associated with

neuroanatomical and neuro-architectural defects in flies, mice and humans. Indeed, mutant flies with reduced Dyrk1A expression present reductions in the volumes of the adult optic lobes and central brain hemispheres (Tejedor et al., 1995). Brains from Dyrk1A heterozygous mice are about 30% smaller and present reduced size and weight in specific brain regions along with reduced neuronal density in the superior colliculus and increased neuronal numbers in brain regions such as somatosensory and motor cortices (Fotaki et al., 2002) with significantly smaller and less complex basal dendritic arbors and reduced dendritic spine densities (Benavides-Piccione et al., 2005). In the hippocampus Dyrk1A heterozygous mice show a significant reduction hippocamppal thickness accompanied by decreases in cell number in CA1, CA2, CA3 and DG (Arqué et al., 2008). Humans with de novo heterozygous variants of DYRK1A also present congenital microcephaly and structural brain abnormalities and intellectual disability (Møller et al., 2008; Ji et al., 2015).

Taken together, our results suggest that combined treatment with EE and EGCG is a potent cognitive enhancing intervention for DS. We demonstrated that EE-EGCG treatment derived cognitive improvements are associated with neuro-modulatory effects at the hippocampus that normalize defects in dendritic spine density and excitatory/inhibitory synaptic puncta ratio. Overall results suggest that combined EE-EGCG treatment has the capacity to simultaneously target several abnormal processes underlying intellectual disability in DS which would be optimal for a disease-modifying intervention in this clinical population.

References

Altafaj X, Dierssen M, Baamonde C, Martí E, Visa J, Guimerà J, Oset M, González JR, Flórez J, Fillat C, Estivill X (2001) Neurodevelopmental delay, motor abnormalities and cognitive deficits in transgenic mice overexpressing Dyrk1A (minibrain), a murine model of Down's syndrome. Hum Mol Genet 10:1915–1924.

652	Antonarakis SE, Lyle R, Dermitzakis ET, Reymond A, Deutsch S (2004) Chromosome 21
653	and down syndrome: from genomics to pathophysiology. Nat Rev Genet 5:725–738.
654	Antonova I, Arancio O, Trillat AC, Wang HG, Zablow L, Udo H, Kandel ER, Hawkins RD
655	(2001) Rapid increase in clusters of presynaptic proteins at onset of long-lasting
656	potentiation. Science 294:1547–1550.
657	Arqué G, Fotaki V, Fernández D, Martínez de Lagrán M, Arbonés ML, Dierssen M (2008)
658	Impaired spatial learning strategies and novel object recognition in mice
659	haploinsufficient for the dual specificity tyrosine-regulated kinase-1A (Dyrk1A). PLoS
660	One 3:e2575.
661	Bain J, McLauchlan H, Elliott M, Cohen P (2003b) The specificities of protein kinase
662	inhibitors: an update. Biochem J 371:199–204.
663	Bains JS, Cusulin JIW, Inoue W (2015) Stress-related synaptic plasticity in the
664	hypothalamus. Nat Rev Neurosci 16:377–388.
665	Bamji SX, Rico B, Kimes N, Reichardt LF (2006) BDNF mobilizes synaptic vesicles and
666	enhances synapse formation by disrupting cadherin-beta-catenin interactions. J Cell
667	Biol 174:289–299.
668	Baroncelli L, Braschi C, Spolidoro M, Begenisic T, Maffei L, Sale A (2011) Brain plasticity
669	and disease: a matter of inhibition. Neural Plast 2011:286073.
670	Bartley AF, Lucas EK, Brady LJ, Li Q, Hablitz JJ, Cowell RM, Dobrunz LE (2015)
671	Interneuron Transcriptional Dysregulation Causes Frequency-Dependent Alterations in
672	the Balance of Inhibition and Excitation in Hippocampus. J Neurosci 35:15276–15290.
673	Becker LE, Armstrong DL, Chan F (1986) Dendritic atrophy in children with Down's
674	syndrome. Ann Neurol 20:520, 526

0/5	Begenisic 1, Spoildoro M, Braschi C, Baroncelli L, Milanese M, Pietra G, Faddri ME,
676	Bonanno G, Cioni G, Maffei L, Sale A (2011) Environmental enrichment decreases
677	GABAergic inhibition and improves cognitive abilities, synaptic plasticity, and visual
678	functions in a mouse model of Down syndrome. Front Cell Neurosci 5:29.
679	Belichenko P V, Kleschevnikov AM, Masliah E, Wu C, Takimoto-Kimura R, Salehi A, Mobley
680	WC (2009) Excitatory-inhibitory relationship in the fascia dentata in the Ts65Dn mouse
681	model of Down syndrome. J Comp Neurol 512:453–466.
682	Belichenko P V, Masliah E, Kleschevnikov AM, Villar AJ, Epstein CJ, Salehi A, Mobley WC
883	(2004) Synaptic structural abnormalities in the Ts65Dn mouse model of Down
684	Syndrome. J Comp Neurol 480:281–298.
685	Benavides-Piccione R, Dierssen M, Ballesteros-Yáñez I, Martínez de Lagrán M, Arbonés
886	ML, Fotaki V, DeFelipe J, Elston GN (2005) Alterations in the phenotype of neocortical
687	pyramidal cells in the Dyrk1A+/- mouse. Neurobiol Dis 20:115–122.
888	Benjamini Y, Hochberg Y (1995) Controlling the False Discovery Rate: A Practical and
689	Powerful Approach to Multiple Testing. J R Stat Soc Ser B 57:289–300.
690	Bhattacharyya A, McMillan E, Chen SI, Wallace K, Svendsen CN (2009) A critical period in
591	cortical interneuron neurogenesis in down syndrome revealed by human neural
692	progenitor cells. Dev Neurosci 31:497–510.
693	Bourne JN, Chirillo MA, Harris KM (2013) Presynaptic ultrastructural plasticity along
694	CA3→CA1 axons during long-term potentiation in mature hippocampus. J Comp Neurol
695	521:3898–3912.
696	Bozdagi O, Shan W, Tanaka H, Benson DL, Huntley GW (2000) Increasing Numbers of
697	Synaptic Puncta during Late-Phase LTP. Neuron 28:245–259.
308	Brown MW, Aggleton, ID (2001) PECOCNITION MEMORY: WHAT ARE THE POLES OF

699	THE PERIRHINAL CORTEX AND HIPPOCAMPUS ? 2.
700	Brown MW, Warburton EC, Aggleton JP (2010) Recognition memory: material, processes,
701	and substrates. Hippocampus 20:1228–1244.
702	Catuara-Solarz S, Espinosa-Carrasco J, Erb I, Langohr K, Notredame C, Gonzalez JR,
703	Dierssen M (2015) Principal Component Analysis of the Effects of Environmental
704	Enrichment and (-)-epigallocatechin-3-gallate on Age-Associated Learning Deficits in a
705	Mouse Model of Down Syndrome. Front Behav Neurosci 9:330.
706	Chakrabarti L, Scafidi J, Gallo V, Haydar TF (2011) Environmental enrichment rescues
707	postnatal neurogenesis defect in the male and female Ts65Dn mouse model of Down
708	syndrome. Dev Neurosci 33:428–441.
709	Chapman RS, Hesketh LJ (2000) Behavioral phenotype of individuals with Down syndrome.
710	Ment Retard Dev Disabil Res Rev 6:84–95.
711	De la Torre R et al. (2014) Epigallocatechin-3-gallate, a DYRK1A inhibitor, rescues cognitive
712	deficits in Down syndrome mouse models and in humans. Mol Nutr Food Res 58:278-
713	288.
714	de la Torre R et al. (2016) Safety and efficacy of cognitive training plus epigallocatechin-3-
715	gallate in young adults with Down's syndrome (TESDAD): a double-blind, randomised,
716	placebo-controlled, phase 2 trial. Lancet Neurol 15:801–810.
717	de Sola S, de la Torre R, Sánchez-Benavides G, Benejam B, Cuenca-Royo A, Del Hoyo L,
718	Rodríguez J, Catuara-Solarz S, Sanchez-Gutierrez J, Dueñas-Espin I, Hernandez G,
719	Peña-Casanova J, Langohr K, Videla S, Blehaut H, Farre M, Dierssen M (2015) A new
720	cognitive evaluation battery for Down syndrome and its relevance for clinical trials.
721	Front Psychol 6:708.
722	Deng W, Aimone JB, Gage FH (2010) New neurons and new memories: how does adult

723	hippocampal neurogenesis affect learning and memory? Nat Rev Neurosci 11:339–350.
724	Diamond DM, Campbell AM, Park CR, Halonen J, Zoladz PR (2007) The temporal dynamics
725	model of emotional memory processing: a synthesis on the neurobiological basis of
726	stress-induced amnesia, flashbulb and traumatic memories, and the Yerkes-Dodson
727	law. Neural Plast 2007:60803.
728	Dias GP, Cavegn N, Nix A, do Nascimento Bevilaqua MC, Stangl D, Zainuddin MSA, Nardi
729	AE, Gardino PF, Thuret S (2012) The role of dietary polyphenols on adult hippocampal
730	neurogenesis: molecular mechanisms and behavioural effects on depression and
731	anxiety. Oxid Med Cell Longev 2012:541971.
732	Dickhaus T (2012) Multiple Comparisons Using R by BRETZ, F., HOTHORN, T., and
733	WESTFALL, P. Biometrics 68:995–995.
734	Dierssen M (2003) Alterations of Neocortical Pyramidal Cell Phenotype in the Ts65Dn
735	Mouse Model of Down Syndrome: Effects of Environmental Enrichment. Cereb Cortex
736	13:758–764.
737	Dierssen M (2012) Down syndrome: the brain in trisomic mode. Nat Rev Neurosci 13:844–
738	858.
739	Escorihuela RM, Ferntidez-teruel A, Vallina IF, Baamonde C, Lumbreras MA, Dierssen M,
740	Tobeha A, Frez J (1995) A behavioral assessment of Ts65Dn mice : a putative Down
741	syndrome model. Neurosci Lett. 199(2):143-146.
742	Fernandez F, Morishita W, Zuniga E, Nguyen J, Blank M, Malenka RC, Garner CC (2007)
743	Pharmacotherapy for cognitive impairment in a mouse model of Down syndrome. Nat
744	Neurosci 10:411–413.
745	Ferrer I, Gullotta F (1990) Down's syndrome and Alzheimer's disease: dendritic spine counts
746	in the hippocampus. Acta Nouropathol 70:690, 695

747	Fotaki V, Dierssen M, Alca S, Martinez S, Casas C, Visa J, Soriano E, Estivill X, Arbone ML
748	(2002) Dyrk1A Haploinsufficiency Affects Viability and Causes Developmental Delay
749	and Abnormal Brain Morphology in Mice. 22:6636–6647.
750	Golabek A, Jarz K, Palminiello S, Walus M, Rabe A, Albertini G (2011) Brain plasticity and
751	environmental enrichment in Ts65Dn mice, an animal model for Down syndrome.
752	Greenacre MJ (2010) Biplots in practice. Wiley Interdiscip Rev Comput Stat 2:613–619.
753	Hand DJ, Taylor CC (1987) Multivariate Analysis of Variance and Repeated Measures: A
754	Practical Approach for Behavioural Scientists. CRC Press.
755	Harris KM, Sultan P (1995) Variation in the number, location and size of synaptic vesicles
756	provides an anatomical basis for the nonuniform probability of release at hippocampal
757	CA1 synapses. Neuropharmacology 34:1387–1395.
758	Harrison FE, Hosseini AH, McDonald MP (2009) Endogenous anxiety and stress responses
759	in water maze and Barnes maze spatial memory tasks. Behav Brain Res 198:247–251.
760	Henningsen A (2011) censReg: censored regression (Tobit) models. R package version 0.5.
761	Hothorn T, Bretz F, Westfall P (2008) Simultaneous Inference in General Parametric Models.
762	Biometrical J 50:346–363.
763	Ji J et al. (2015) DYRK1A haploinsufficiency causes a new recognizable syndrome with
764	microcephaly, intellectual disability, speech impairment, and distinct facies. Eur J Hum
765	Genet 23:1473–1481.
766	Jia N, Han K, Kong J-J, Zhang X-M, Sha S, Ren G-R, Cao Y-P (2013) (-)-Epigallocatechin-3-
767	gallate alleviates spatial memory impairment in APP/PS1 mice by restoring IRS-1
768	signaling defects in the hippocampus. Mol Cell Biochem 380:211–218.
769	Khoshnood B, Greenlees R, Loane M, Dolk H (2011) Paper 2: EUROCAT public health

770	indicators for congenital anomalies in Europe. Birth Defects Res A Clin Mol Teratol 91
771	Suppl 1:S16–S22.
772	Kleschevnikov AM, Belichenko P V, Faizi M, Jacobs LF, Htun K, Shamloo M, Mobley WC
773	(2012) Deficits in cognition and synaptic plasticity in a mouse model of Down syndrome
774	ameliorated by GABAB receptor antagonists. J Neurosci 32:9217–9227.
775	Lê S, Josse J, Husson F (2008) FactoMineR: An R Package for Multivariate Analysis. J Stat
776	Softw 25:1–18.
777	Leger M, Quiedeville A, Bouet V, Haelewyn B, Boulouard M, Schumann-Bard P, Freret T
778	(2013) Object recognition test in mice. Nat Protoc. 8(12):2531-7. doi:
779	10.1038/nprot.2013.155. Epub 2013 Nov 21.
780	Li Q, Zhao HF, Zhang ZF, Liu ZG, Pei XR, Wang JB, Cai MY, Li Y (2009a) Long-term
781	administration of green tea catechins prevents age-related spatial learning and memory
782	decline in C57BL/6 J mice by regulating hippocampal cyclic amp-response element
783	binding protein signaling cascade. Neuroscience 159:1208–1215.
784	Li Q, Zhao HF, Zhang ZF, Liu ZG, Pei XR, Wang JB, Li Y (2009b) Long-term green tea
785	catechin administration prevents spatial learning and memory impairment in
786	senescence-accelerated mouse prone-8 mice by decreasing Abeta1-42 oligomers and
787	upregulating synaptic plasticity-related proteins in the hippocampus. Neuroscience
788	163:741–749.
789	Lott IT, Dierssen M (2010) Cognitive deficits and associated neurological complications in
790	individuals with Down's syndrome. Lancet Neurol 9:623–633.
791	Maei HR, Zaslavsky K, Teixeira CM, Frankland PW (2009) What is the Most Sensitive
792	Measure of Water Maze Probe Test Performance? Front Integr Neurosci 3:4.
793	Mahoney G, Wheeden CA, Perales F (2004) Relationship of preschool special education

794	outcomes to instructional practices and parent-child interaction. Res Dev Disabil
795	25:539–558.
796	Martinez de Lagran M, Benavides-Piccione R, Ballesteros-Yañez I, Calvo M, Morales M,
797	Fillat C, Defelipe J, Ramakers GJ a, Dierssen M (2012) Dyrk1A influences neuronal
798	morphogenesis through regulation of cytoskeletal dynamics in mammalian cortical
799	neurons. Cereb Cortex 22:2867–2877.
800	Martínez-Cué C, Baamonde C, Lumbreras M, Paz J, Davisson MT, Schmidt C, Dierssen M,
801	Flórez J (2002) Differential effects of environmental enrichment on behavior and
802	learning of male and female Ts65Dn mice, a model for Down syndrome. Behav Brain
803	Res 134:185–200.
804	Martinez-Cue C, Martinez P, Rueda N, Vidal R, Garcia S, Vidal V, Corrales a., Montero J a.,
805	Pazos a., Florez J, Gasser R, Thomas a. W, Honer M, Knoflach F, Trejo JL, Wettstein
806	JG, Hernandez M-C (2013) Reducing GABAA 5 Receptor-Mediated Inhibition Rescues
807	Functional and Neuromorphological Deficits in a Mouse Model of Down Syndrome. J
808	Neurosci 33:3953–3966.
809	Møller RS, Kübart S, Hoeltzenbein M, Heye B, Vogel I, Hansen CP, Menzel C, Ullmann R,
810	Tommerup N, Ropers H-H, Tümer Z, Kalscheuer VM (2008) Truncation of the Down
811	syndrome candidate gene DYRK1A in two unrelated patients with microcephaly. Am J
812	Hum Genet 82:1165–1170.
813	Nadel L (2003) Down's syndrome: a genetic disorder in biobehavioral perspective. Genes
814	Brain Behav 2:156–166.
815	Netzer WJ, Powell C, Nong Y, Blundell J, Wong L, Duff K, Flajolet M, Greengard P (2010)
816	Lowering beta-amyloid levels rescues learning and memory in a Down syndrome
817	mouse model. PLoS One 5:e10943

818	Ortiz-López L, Márquez-Valadez B, Gómez-Sánchez A, Silva-Lucero MDC, Torres-Pérez M,
819	Téllez-Ballesteros RI, Ichwan M, Meraz-Ríos MA, Kempermann G, Ramírez-Rodríguez
820	GB (2016) Green tea compound epigallo-catechin-3-gallate (EGCG) increases neuronal
821	survival in adult hippocampal neurogenesis in vivo and in vitro. Neuroscience 322:208-
822	220.
823	Parker SE, Mai CT, Canfield MA, Rickard R, Wang Y, Meyer RE, Anderson P, Mason CA,
824	Collins JS, Kirby RS, Correa A (2010) Updated National Birth Prevalence estimates for
825	selected birth defects in the United States, 2004-2006. Birth Defects Res A Clin Mol
826	Teratol 88:1008–1016.
827	Pennington BF, Moon J, Edgin J, Stedron J, Nadel L (2003) The Neuropsychology of Down
828	Syndrome: Evidence for Hippocampal Dysfunction. Child Dev 74:75–93.
829	Pinheiro J, Bates D, DebRoy S, Sarkar D, R Core Team (2016) {nlme}: Linear and Nonlinear
830	Mixed Effects Models.
831	Pons-Espinal M, Martinez de Lagran M, Dierssen M (2013) Environmental enrichment
832	rescues DYRK1A activity and hippocampal adult neurogenesis in TgDyrk1A. Neurobiol
833	Dis 60:18–31.
834	Ramírez-Rodríguez G, Ocaña-Fernández MA, Vega-Rivera NM, Torres-Pérez OM, Gómez-
835	Sánchez A, Estrada-Camarena E, Ortiz-López L (2014) Environmental enrichment
836	induces neuroplastic changes in middle age female Balb/c mice and increases the
837	hippocampal levels of BDNF, p-Akt and p-MAPK1/2. Neuroscience 260:158–170.
838	Reeves RH, Irving NG, Moran TH, Wohn A, Kitt C, Sisodia SS, Schmidt C, Bronson RT,
839	Davisson MT (1995) A mouse model for Down syndrome exhibits learning and
840	behaviour deficits. Nat Genet 11:177–184.
841	Reynolds GP, Warner CE (1988) Amino acid neurotransmitter deficits in adult Down's

842	syndrome brain tissue. Neurosci Lett 94:224–227.
843	Risser D, Lubec G, Cairns N, Herrera-Marschitz M (1997) Excitatory amino acids and
844	monoamines in parahippocampal gyrus and frontal cortical pole of adults with Down
845	syndrome. Life Sci 60:1231–1237.
846	Sale A, Berardi N, Maffei L (2014) Environment and brain plasticity: towards an endogenous
847	pharmacotherapy. Physiol Rev 94:189–234.
848	Seidl R, Cairns N, Lubec G (2001) The brain in Down syndrome. J Neural Transm
849	Suppl:247–261.
850	Sham PC, Purcell SM (2014) Statistical power and significance testing in large-scale genetic
851	studies. Nat Rev Genet 15:335–346.
852	Souchet B, Guedj F, Penke-Verdier Z, Daubigney F, Duchon A, Herault Y, Bizot J-C, Janel
853	N, Créau N, Delatour B, Delabar JM (2015) Pharmacological correction of
854	excitation/inhibition imbalance in Down syndrome mouse models. Front Behav Neurosci
855	9.
856	Tejedor F, Zhu XR, Kaltenbach E, Ackermann A, Baumann A, Canal I, Heisenberg M,
857	Fischbach KF, Pongs O (1995) minibrain: a new protein kinase family involved in
858	postembryonic neurogenesis in Drosophila. Neuron 14:287–301.
859	Tsien JZ, Huerta PT, Tonegawa S (1996) The Essential Role of Hippocampal CA1 NMDA
860	Receptor–Dependent Synaptic Plasticity in Spatial Memory. Cell 87:1327–1338.
861	Whishaw IQ, Jarrard LE (1996) Evidence for extrahippocampal involvement in place learning
862	and hippocampal involvement in path integration. Hippocampus 6:513–524.
863	Wickham H (2009) ggplot2: elegant graphics for data analysis. Springer New York.
864	Xie W, Ramakrishna N, Wieraszko A, Hwang Y-W (2008) Promotion of neuronal plasticity by

866	Young D, Lawlor PA, Leone P, Dragunow M, During MJ (1999) Environmental enrichmen
867	inhibits spontaneous apoptosis, prevents seizures and is neuroprotective. Nat Med
868	5:448–453.

(-)-epigallocatechin-3-gallate. Neurochem Res 33:776-783.

869

870

871

872

873

874

875

876

877

878

879

880

881

882

883

884 885

886

887

888

889

865

Figure legends

Figure 1. EE-EGCG treatment effects on young Ts65Dn mice deficits in spatial learning, reference memory and cognitive flexibility. (A) Heat-map representing the accumulated swimming trajectories of mice from the different experimental groups across acquisition, removal and reversal sessions in the MWM. Periphery and center zones are depicted in the upper left plot. The color code is represented on the right, with red corresponding to the most visited zones and black to the less or non-visited zones. Learning curves are represented in: (B) Latency (s) to reach the escape platform (C) Gallagher distance (accumulated distance to the goal in cm) and (D) Thigmotaxis (percentage of time spent on the periphery) during the acquisition sessions. (E and F) Boxplots of the distribution of the Latency to the first entry to the platform area and the Gallagher distance of the four experimental groups in the removal session. Dots indicate the values of each individual mouse. Reversal learning curves are represented in: (G) Latency (s), (H) Gallagher distance and (I) Thigmotaxis. Abbreviations: A1-5 = acquisition sessions 1-5; R1-3 = reversal sessions 1-3 with 4 trials per day; REM = removal session. Data in B, C, D, F, G and H are represented as mean ± SEM. Data in B and F were analyzed by a censored model, which considered 60 s as the maximum trial duration. Data in C, D, G and H were analyzed with ANOVA repeated measures and data in E were analyzed by one-way ANOVA. In all cases Tukey multiple post-hoc comparisons corrected with BH were employed. Even if all groups were considered for multiple comparisons the figure reports only statistically significant

893

894

895

896

897

898

899

900

901

902

903

904

905

906

907

908

909

910

911

912

913

914

915

916

differences of the following relevant contrasts of interest: WT vs. TS; TS vs. TS EE-EGCG;

WT vs. TS EE-EGCG (* p < 0.05, ** p < 0.01, *** p < 0.001).

Figure 2. Supervised PCA of the experimental groups during the acquisition sessions revealed that EE-EGCG treatment improves global learning in Ts65Dn mice. (A) Trajectories connect group performance (medians) along the five learning sessions (labeled with its respective number) in the space defined by the first and second principal components (PC1 and PC2), which consist of linear combinations of the original variables. (B) Variable directionality in the PCA space. Arrows represent the direction with respect to PC1 and PC2. Variables reaching the unit circle belong to variables that are well represented by the two principal components. (C) Contribution of variables to PC1 and (D) PC2 (in percent). The first principal component receives a similar contribution from all classical variables used to assess learning and can thus be understood as a composite learning variable. (E) Boxplots of PC1 distribution for each experimental group on first and fifth session of the acquisition phase. Boxplot horizontal lines represent the group median, box edges the 25th and 75th percentiles and the whiskers correspond minimum and maximum values to a maximum of 1.5 times the interquartile distance from the box. More extreme values are individually plotted. Only relevant comparisons are reported in the figure for the sake of clarity (WT vs. TS; TS vs. TS EE-EGCG; WT vs. TS EE-EGCG) even if all groups were considered for the permutation test (* p < 0.05, ** p < 0.01, *** p < 0.001). The benefits of the EE-EGCG treatment on Ts65Dn learning explain the displacement of this group towards more positive values along the PC1.

Figure 3. Supervised PCA of the experimental groups during the reversal sessions revealed poorer cognitive flexibility on untreated Ts65Dn mice. (A) Trajectories of medians along the reversal session (accordingly labeled) on the space formed by the first and second principal components (PC1 and PC2). (B) Variable directions on the PCA space defined by PC1 and PC2. Variables reaching the unit circle belong to variables that are well represented by the two principal components. (C) Barplots represent the contribution of

variables in percentage to PC1 and **(D)** PC2. **(E)** Boxplots of PC1 distribution for each experimental group on first and third session of the reversal phase. Boxplot horizontal lines represent the group median, box edges the 25th and 75th percentiles and the whiskers correspond minimum and maximum values to a maximum of 1.5 times the interquartile distance from the box. More extreme values are individually plotted. Only relevant comparisons are reported in the figure for the sake of clarity (WT vs. TS; TS vs. TS EE-EGCG; WT vs. TS EE-EGCG) even if all groups were considered for the permutation test (* p < 0.05, ** p < 0.01,*** p < 0.001). The shift of mice groups towards positive values of PC1 represents the increased cognitive flexibility of the groups, with treated TS attaining higher values than their untreated counterpart.

Figure 4. Effect of treatment on the discrimination index (DI) in the novel object recognition test. Left panel shows a diagram of the apparatus used for the novel object recognition test. Right panel depicts the boxplots of the distribution of the DI (%) among the experimental groups. Dots indicate the DI measure from each individual mouse, dashed lines indicate group means and continuous lines indicate group medians. Data were analyzed using one-way ANOVA, and Tukey multiple post-hoc comparisons corrected with BH. Even if all groups were considered for multiple comparisons the figure reports only statistically significant differences of the following relevant contrasts of interest: WT vs. TS; TS vs. TS EE-EGCG; WT vs. TS EE-EGCG (* p < 0.05; ** p < 0.01). Ts65Dn mice show a trend towards a reduction in DI (p= 0.08). EE-EGCG treatment improves DI score in Ts65Dn mice but worsens performance in WT mice.

Figure 5. Ts65Dn mice show a reduction in dendritic spine density in DG and CA1 and EE-EGCG treatment ameliorates this deficit in CA1. Left: panel showing the dorsal hippocampal region of a Golgi preparation illustrating dendrites from CA1 and DG subregions scale bar represents 10 μ m. Figures A) and B) show boxplots of the distribution of dendritic spine density (spines per μ m) in DG and CA1 among the experimental groups. Dots indicate the repeated values from individual mice (2-3 dendrites per slice, 3 dorsal

hippocampal slices per brain, 5-6 mice per experimental group), dashed lines indicate group means and continuous lines indicate group medians. Data were analyzed with a linear mixed model, which included the experimental group as a factor and mouse as a random effect. F-test was used to test the global hypothesis. Post-hoc tests were applied for the following contrasts of interest: WT vs. TS; TS – TS EE-EGCG and WT vs. WT-EE-EGCG (* p < 0.05; *** p < 0.001). Ts65Dn mice show a significant reduction in spine density both in DG and CA1. EE-EGCG treatment increases dendritic spine density in CA1. In Ts65Dn, and decreases this parameter in WT.

Figure 6. EE-EGCG effects on VGLUT1 / VGAT puncta in DG and CA1. The figure shows boxplots of the distribution of VGLUT1 / VGAT ratio of different puncta density and percentage of area among the experimental groups at DG and CA1. A) and C) show VGLUT1 / VGAT ratio of puncta density (puncta per μ m²), B) and D) show VGLUT1 / VGAT ratio of % of area occupied. Dots indicate the repeated values from individual mice, dashed lines indicate group means and continued lines indicate group medians. Data were analyzed with a linear mixed model which included the experimental group as a factor and mouse as a random effect. F-test was used to test the global hypothesis. Post-hoc tests were applied for the following contrasts of interest: WT vs. TS; TS – TS EE-EGCG and WT vs. WT-EE-EGCG (* p < 0.05; ** p < 0.01, *** p < 0.001).

Statistical Tables

Table 1: Single-variate MWM multiple post-hoc comparisons with BH correction

Figure Var	M. C.H.	DI			- · · · · · · · · · · · · · · · · · · ·	Estimated	Sd	95	% CI	
	Variable	Phase	Contrast	Data structure	Type of test	mean difference	error	Lower	Higher	p-value
Fig.1B	Latency	ACQ	Overall effect	Continuous variable	Tobit model	$\chi^2_{(3)}=42,24$	1	1	1	<0,001
Fig.1B	Latency	ACQ	TS_WT	Continuous variable	Tobit model	51,262	11,28	29,146	73,377	<0,001

Fig.1B	Latency	ACQ	TS EE- EGCG_TS	Continuous variable	Tobit model	-23,839	12,98	-49,280	1,602	0,028
Fig.1B	Latency	ACQ	TS EE- EGCG_W T	Continuous variable	Tobit model	27,423	11,40	5,066	49,780	0,005
Fig.1C	Gallagher distance	ACQ	Overall effect	Continuous variable	Anova repeated measures F-test	F=13,636	-	1	-	<0,0001
Fig.1C	Gallagher distance	ACQ	TS_WT	Continuous variable	Anova repeated measures F-test	1903,3	397,6	1124	2682,6	<0,001
Fig.1C	Gallagher distance	ACQ	TS EE- EGCG_ TS	Continuous variable	Anova repeated measures F-test	-896,3	427,9	-1734,9	-57,6	0,043
Not shown	Gallagher index	ACQ	Overall effect	Continuous variable	Anova repeated measures F-test	F=10,226	-	-	-	<0,001
Not shown	Gallagher index	ACQ	TS_WT	Continuous variable	Anova repeated measures F-test	17,217	3,981	9,41424	25,01976	<0,001
Not shown	Gallagher index	ACQ	TS EE- EGCG _TS	Continuous variable	Anova repeated measures F-test	-8,903	4,284	-17,2996	-0,50636	0,045
Fig.1D	Thigmotaxis	ACQ	Overall effect	Continuous variable	Anova repeated measures F-test	F=9,22	-	-	-	<0,001
Fig.1D	Thigmotaxis	ACQ	TS_WT	Continuous variable	Anova repeated measures F-test	21,172	5,629	10,13916	32,20484	<0,001
Fig.1D	Thigmotaxis	ACQ	TS EE- EGCG _TS	Continuous variable	Anova repeated measures F-test	-11,374	6,057	-23,2457	0,49772	0,09
Not shown	Speed	ACQ	Overall effect	Continuous variable	Anova repeated measures F-test	F=4,883	-	-	-	0,006
Not shown	Speed	ACQ	TS_WT	Continuous variable	Anova repeated measures F-test	-4,547	1,354	-7,20084	-1,89316	0,0047
Not shown	Speed	ACQ	TS_TS EE- EGCG	Continuous variable	Anova repeated measures F-test	1,725	1,457	-1,13072	4,58072	0,28
Not shown	Speed	ACQ	WT EE- EGCG _WT	Continuous variable	Anova repeated measures F-test	-0,485	1,216	-2,86836	1,89836	0,69
Fig.1E	Latency first entry	REM	TS_WT	Continuous variable	One- way Anova	25,284	7,295	10,9858	39,5822	0,0042
Fig.1E	Latency first entry	REM	TS EE- EGCG _TS	Continuous variable	One- way Anova	-16,075	7,850	-31,461	-0,689	0,096
Fig.1F	Latency first entry	REM	Overall effect	Continuous variable	One- way Anova	F=6,159	-	1	1	0,002
Fig.1F	Gallagher index	REM	TS_WT	Continuous variable	One- way Anova	17,991	7,041	4,19064	31,79136	0,03
Fig.1F	Gallagher distance	REM	TS_WT	Continuous variable	One- way Anova	1272,4	455,5	-437,28	2165,18	0,02520
Fig.1F	Gallagher index	REM	TS EE- EGCG _TS	Continuous variable	One- way Anova	-11,944	7,577	-26,7949	2,90692	0,14
Fig.1G	Latency	REV	Overall effect	Continuous variable	Tobit model	$\chi^2_{(3)}= 26,59$	-	-	-	<0,001
Fig.1G	Latency	REV	TS_WT	Continuous variable	Tobit model	35,093	9,16	17,124	53,063	<0,001
Fig.1G	Latency	REV	TS EE- EGCG _TS	Continuous variable	Tobit model	-14,865	9,28	-33,073	3,342	0,060
Fig.1H	Gallagher distance	REV	Overall effect	Continuous variable	Anova repeated measures F-test	F=7,694	-	-	-	<0,001
Fig.1H	Gallagher distance	REV	TS_WT	Continuous variable	Anova repeated measures F-test	2114,3	412	1306,78	2921,82	<0,001
Fig.1H	Gallagher distance	REV	TS EE- EGCG _TS	Continuous variable	Anova repeated measures F-test	-869	443,3	-1737,87	-0,132	0,059
Not shown	Gallagher index	REV	Overall effect	Continuous variable	Anova repeated measures F-test	F=11,714	-	-	-	<0,001

Not shown	Gallagher index	REV	TS_WT	Continuous variable	Anova repeated measures F-test	20,8045	4,310 2	12,35651	29,25249	<0,001
Not shown	Gallagher index	REV	TS EE- EGCG _TS	Continuous variable	Anova repeated measures F-test	-6,3488	4,638	-15,4393	2,74168	0,2
Fig.1H	Thigmotaxis	REV	Overall effect	Continuous variable	Anova repeated measures F-test	F=10,105	-	1		<0,001
Fig.1H	Thigmotaxis	REV	TS_WT	Continuous variable	Anova repeated measures F-test	21,393	6,268	9,10772	33,67828	0,00129
Fig.1H	Thigmotaxis	REV	TS EE- EGCG _TS	Continuous variable	Anova repeated measures F-test	-9,867	6,745	-23,0872	3,3532	0,14
Not shown	Speed	REV	Overall effect	Continuous variable	Anova repeated measures F-test	F=2,607	-	-	-	0,067

970 Table 2: Multivariate within-group variances before and after learning, acquisition and

971 reversal sessions Within-group variances of experimental groups (sum over squared

972 distances from group barycentre divided by group size, scaled by number of variables).

Figure	Session	WT	WTEEEGCG	TS	TSEEEGCG
2E	ACQ1	0,42	0,89	0,24	0,53
2E	ACQ5	1,62	1,55	0,87	0,95
3E	REV1	1,52	1,12	0,56	1,22
3E	REV3	2,68	1,84	1,42	2,26

973

974 Table 3: Permutation-test results of learning related composite measure PC1

Figure	Variable	Phase	Contrast	Pseudo-t	p-value
rigure	Variable	Filase	Contrast	rseuuo-t	p-value
2E	PC1	ACQ1	TS_WT	3,67	<0,001
2E	PC1	ACQ1	TS_WT EE-EGCG	3,57	<0,001
2E	PC1	ACQ1	TS_TS EE-EGCG	3,05	0,004
2E	PC1	ACQ1	TS EE-EGCG_WT	0,28	0,39
2E	PC1	ACQ1	TS EE-EGCG_WT EE-EGCG	0,54	0,71
2E	PC1	ACQ1	WT_WT EE-EGCG	0,8	0,89
2E	PC1	ACQ5	TS_WT	6,81	<0,001
2E	PC1	ACQ5	TS_WT EE-EGCG	6,72	<0,001
2E	PC1	ACQ5	TS_TS EE-EGCG	1,85	0,045
2E	PC1	ACQ5	TS EE-EGCG_WT	5,2	9,99
2E	PC1	ACQ5	TS EE-EGCG_WT EE-EGCG	5,06	<0,001
2E	PC1	ACQ5	WT_WT EE-EGCG	0,27	0,39
3E	PC1	REV1	TS_WT	4,60	<0,001
3E	PC1	REV1	TS_WT EE-EGCG	5,60	<0,001
3E	PC1	REV1	TS_TS EE-EGCG	2,59	0,01

3E	PC1	REV1	TS EE-EGCG_WT	2,44	0,01
3E	PC1	REV1	TS EE-EGCG_WT EE-EGCG	3,07	0,005
3E	PC1	REV1	WT_WT EE-EGCG	0,23	0,58
3E	PC1	REV3	TS_WT	5,17	<0,001
3E	PC1	REV3	TS_WT EE-EGCG	6,19	<0,001
3E	PC1	REV3	TS_TS EE-EGCG	2,32	0,02
3E	PC1	REV3	TS EE-EGCG_WT	2,66	0,01
3E	PC1	REV3	TS EE-EGCG_WT EE-EGCG	3,21	0,004
3E	PC1	REV3	WT_WT EE-EGCG	0,21	0,58

976 Table 4: Novel object recognition test (Discrimination Index)

				Estimated	95%	6 CI	
Figure	Contrast	Data structure	Type of test	mean difference	Lower	Higher	p-value
4	TS _WT	Continuous variable	ANOVA	-21,728	-42,94	-0,511	0,083
4	TS EE-EGCG_TS	Continuous variable	ANOVA	27,224	5,311	49,136	0,044
4	TS EE-EGCG _WT	Continuous variable	ANOVA	5,496	-15,721	26,713	0,616
4	WT EE-EGCG_WT	Continuous variable	ANOVA	-42,928	-64,145	-21,711	0,001

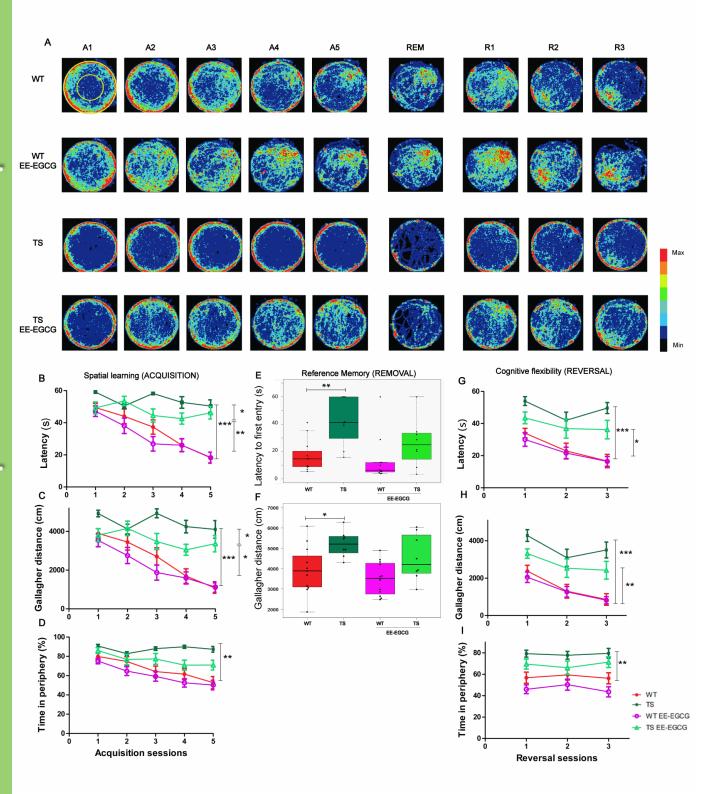
Table 5: Dendritic Spine density

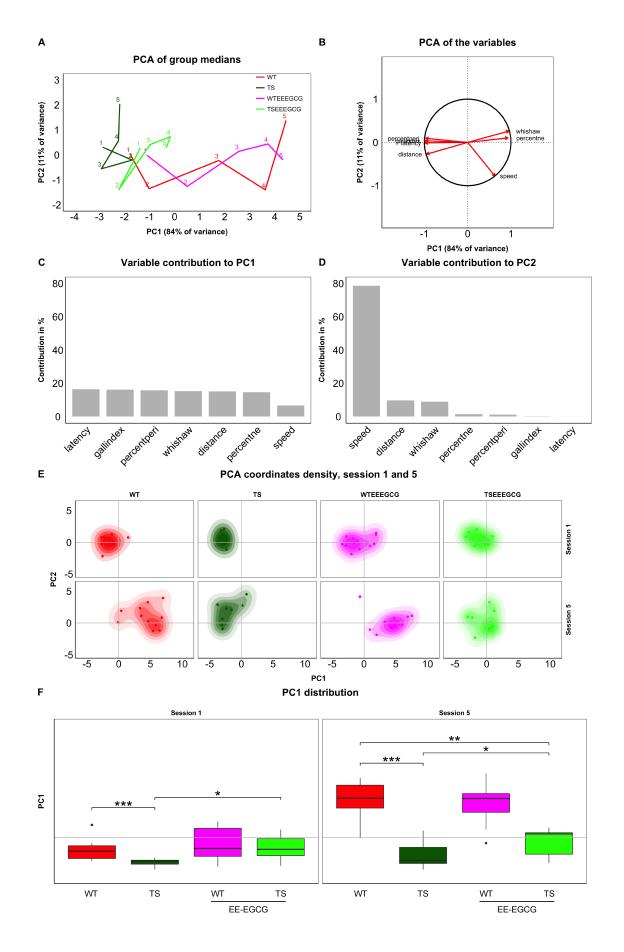
					Estimated	95%	6 CI	
Figure	Region	Contrast	Data structure	Type of test	mean difference	Lower	Higher	p-value
5A	DG	TS _WT	Continuous variable	Mixed model F-test	-0,192	-0,383	-0,002	0,048
5B	CA1	TS _WT	Continuous variable	Mixed model F-test	-0,175	-0,282	-0,069	< 0,001
5B	CA1	TS EE-EGCG_TS	Continuous variable	Mixed model F-test	0,105	0,001	0,209	0,047
5B	CA1	WT EE-EGCG_WT	Continuous variable	Mixed model F-test	-0,129	-0.234	-0,025	0,01

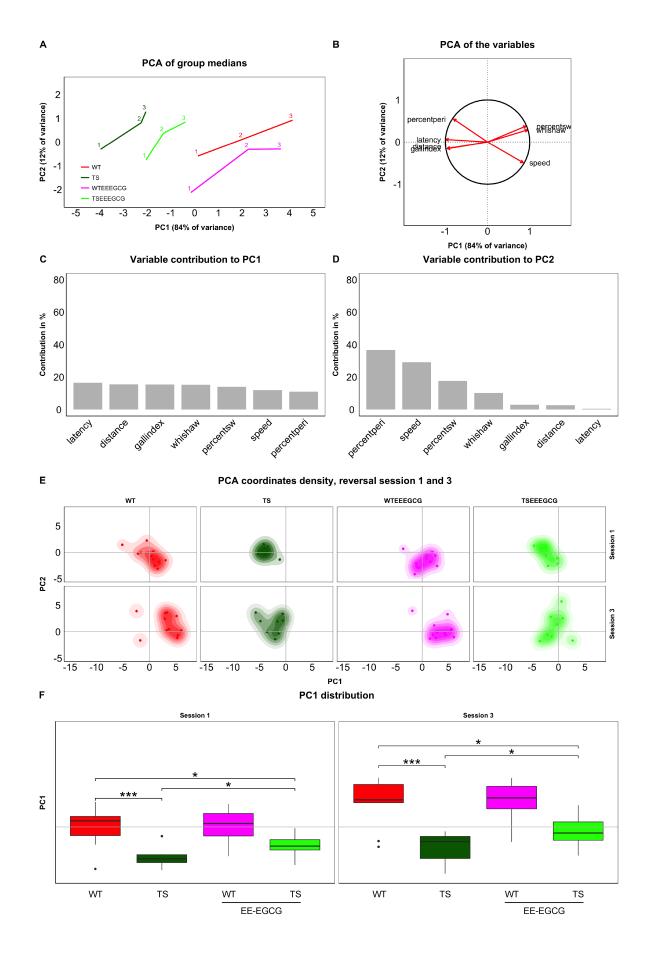
Table 6: VGLUT1 and VGAT synaptic puncta

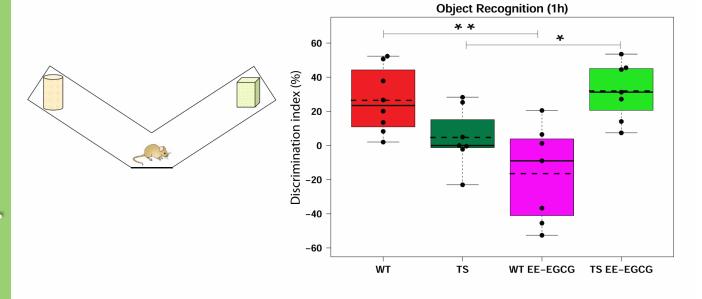
						Estimated	95% CI		
Figure	Variable	Region	Contrast	Data structure	Type of test	mean difference	Lower	Higher	p-value
	VGLUT1 puncta			Continuous	Mixed model				
Not shown	density	DG	TS _WT	variable	F-test	0,077	0,018	0,136	0,006
				Continuous	Mixed model				
Not shown	VGLUT1 puncta size	DG	TS _WT	variable	F-test	-0,06	-0,098	-0,022	0,001
	VGLUT1/VGAT			Continuous	Mixed model				
6A	puncta density	DG	TS _WT	variable	F-test	0,308	0,151	0,465	< 0,001

	VGLUT1/VGAT % of			Continuous	Mixed model		Ì		
6B	area	DG	TS _WT	variable	F-test	0,077	-0,03	0,183	0,222
	VGLUT1puncta		TS EE-	Continuous	Mixed model				
Not shown	density	DG	EGCG_TS	variable	F-test	-0,073	-0,132	-0,014	0,01
			TS EE-	Continuous	Mixed model				
Not shown	VGLUT1 puncta size	DG	EGCG_TS	variable	F-test	0,06	0,022	0,098	0,001
	VGLUT1/VGAT		TS EE-	Continuous	Mixed model				
6A	puncta density	DG	EGCG_TS	variable	F-test	-0,294	-0,452	-0,137	< 0,001
	VGLUT1 puncta			Continuous	Mixed model				
Not shown	density	CA1	TS _WT	variable	F-test	0,071	0,008	0,134	0,022
				Continuous	Mixed model				
Not shown	VGLUT1 puncta size	CA1	TS _WT	variable	F-test	-0,093	-0,145	-0,041	0,043
				Continuous	Mixed model				
Not shown	VGAT puncta size	CA1	TS _WT	variable	F-test	0,054	0,001	0,106	0,043
	VGLUT1/VGAT			Continuous	Mixed model				
6C	puncta density	CA1	TS _WT	variable	F-test	0,295	0,098	0,493	0,001
	VGLUT1/VGAT % of			Continuous	Mixed model				
6D	area	CA1	TS _WT	variable	F-test	-0,145	-0,275	-0,016	0,023
	VGLUT1/VGAT		TS EE-	Continuous	Mixed model				
6C	puncta density	CA1	EGCG_TS	variable	F-test	-0,245	-0,442	-0,047	0,01
			WT EE-	Continuous	Mixed model				
Not shown	VGAT puncta size	CA1	EGCG_WT	variable	F-test	0,049	-0,003	0,102	0,07
	VGLUT1/VGAT % of		WT EE-	Continuous	Mixed model				
6D	area	CA1	EGCG_WT	variable	F-test	-0,137	-0,267	-0,007	0,035









CA1

Dendritic spine density

